

Effects of Parton Dynamics on Neutral Pion Distributions at RHIC energies

Y. Nara

RIKEN-BNL Research Center, Brookhaven Nation Laboratory, Upton, NY

S.E. Vance

Physics Department, Brookhaven Nation Laboratory, Upton, NY

P. Csizmadia

RMKI Research Institute for Particle and Nuclear Physics, Budapest, Hungary

We study the π^0 transverse momentum distributions in Au+Au at RHIC within a transport theoretical approach for mini-jet partons which are produced from the initial hard scattering. Two different hadronization models are used to obtain hadrons. Dynamical approach with inelastic parton-parton interactions reproduces the recent RHIC data on π^0 spectra with a parton scattering cross sections of about 5-12mb depending on the hadronization model. We discuss the parton cross section as well as the energy loss parameter dE/dz dependence on π^0 spectra and hadron multiplicities.

25.75.-q, 12.38.Mh, 24.85.+p, 13.87.-a

Recently, high p_T neutral pion production in the $1.0 < p_T < 4.0$ GeV/c transverse momentum range at RHIC are reported [1]. At collider energies, it has been argued that the contribution of hard scattering becomes important [2]. In the case of heavy ion collisions, (mini-)jets which are produced from the primarily hard scattering of partons should travel through the dense matter. Therefore, final hadron jet spectra would be suppressed comparison to the pp collisions due to the loss of energies. This phenomenon called "jet quenching" has been proposed to one of the promising signatures for the quark-gluon plasma (QGP) [3-5]. PHENIX data shows that π^0 spectra for peripheral collisions are explained by $p\bar{p}$ data taking account of the number of binary collision, while spectra for the central collisions shows the suppression comparison to the simple scaling. Some theoretical calculations also suggest that inclusion of parton energy loss is necessary to explain the data. The difference of the large p_T distributions from the pQCD motivated extrapolations has been interpreted as evidence of jet quenching [6].

The HIJING simulation model [7] and several of its variants such as AMPT [9] and HIJING/B \bar{B} [8] incorporate a simple jet quenching mechanism. The algorithm which attempts to describe the energy loss predicts a large and non-linear increase in the hadron multiplicity with high energy [10]. However, recent Data on the multiplicity is only linear and thus does not have this non-linear behavior [11,12]. In this work, we will argue that dynamical effects is important to understand the mechanism of the parton energy loss.

Kinetic theory based on the Boltzmann equation has been extensively applied in order to understand the time evolution of strongly interacting partonic matter that is formed in the high energy nuclear collisions. To get the appropriate solution of the Boltzmann equation, the relaxation time approximation [13] or, recently, Landau

equation have been used [14]. Monte Carlo type simulation methods have been also developed to solve the Boltzmann equation for partons [15-18].

In the most of the parton transport approach, such as the ZPC [16], AMPT [21,9], and MPC [17], the dynamical effects of the elastic parton-parton scattering have been studied within the HIJING initial conditions (gluon number $dN_g/dy \approx 200$ near mid-rapidity). The partonic effects are hard to be seen on the hadronic multiplicity or elliptic flow when the only elastic parton-parton collisions with the typical gluon-gluon pQCD cross section of $\sigma_{gg} \sim 3$ mb is taken into account in the model. It is suggested that inelastic processes like $gg \rightarrow ggg$ should be important [19,20] for thermalization as well as energy loss of partons. The purpose of the present study is to understand the role of the parton dynamics on the pion transverse spectra based on the transport approach with the Bremsstrahlung in the parton scattering.

It is of most important to have the true knowledge about the initial conditions for the subsequent evolutions of parton system produced in the early stage of heavy ion collisions. The initial conditions for the time evolution of the partons in heavy ion collisions at collider energies proposed so far would be divided roughly by three models; 1) mini-jets + final state saturation by K. Eskola *et al.* [31], 2) string + mini-jets initial condition by HIJING [7], 3) initial parton saturation [32] and soft partons from classical Yang-Mills field [33,34]. We take the HIJING mini-jet initial conditions for subsequent parton evolution in this work to see clearly the dynamical effects comparing the HIJING model.

Our approach is based on the Relativistic Boltzmann Equation for the time evolution of the system,

$$p \cdot \partial f_i(x^\mu, p^\mu) = C_i, \quad (1)$$

where f_i is the one-particle distribution function for

quarks, antiquarks and gluons and C_i is the collision integral. We assume that, for the collision integral, the $2 \rightarrow 2$ collisions as well as the $2 \rightarrow 2 + \text{Bremsstrahlung}$ are considered. Technically, Radiations are accomplished by adding final state radiation as in the PYTHIA algorithms [23]. The long-range color force is not included in this simulation. However, we note that there are some models to try to include mean field part into kinetic theory [24].

In the solution of the Boltzmann equation, the one-particle distribution function, $f(x, p)$ is assumed to be the sum of point particles,

$$f(x, p) = \frac{1}{N_{test}} \sum_{i=1}^{AN_{test}} \delta(x_i - x) \delta(p_i - p), \quad (2)$$

where N_{test} is the number of “test particle” and A is the actual number of particles, respectively.

There are some numerical methods to simulate the collision integral of the Boltzmann equation in a Monte-Carlo fashion. One of the computational schemes are “closest distance approach” which is also called “parallel-ensemble” method. if the minimum relative distance b_{rel} for any pair of particles in their c.m. system becomes less than interaction range specified by $\sqrt{\sigma(\sqrt{s})}/\pi$, where $\sigma(\sqrt{s})$ is the total parton-parton cross section for the pair at the c.m. energy of \sqrt{s} , then partons are assumed to collide. This method has been widely used to simulate the low energy nucleus-nucleus collisions [25]. However, this method violates Lorentz invariance due to the nature of action at a distance. Distribution function in the Boltzmann collision integral should be taken at the same space-time point. Those problems have been studied by several authors [16–18,30]. In contrast, “full-ensemble” method in which each test particle interact with a reduced cross section σ/N_{test} has been used [26,27,17]. In the limit of $N_{test} \rightarrow \infty$, one obtains the locality in configuration space. Another interesting method is “local-ensemble” method [28,29] where the probability for one pair of test particles to collide during the time interval of Δt in the small volume element ΔV is given by

$$W = \sigma v \Delta t / (N_{test} \Delta V). \quad (3)$$

Here v is the relative velocity of the scattering particles. In the limit of $\Delta V \rightarrow 0$, $\Delta t \rightarrow 0$, $N_{test} \rightarrow \infty$, the solutions will converge to the exact solutions of the Boltzmann equation. In this study, we use full-ensemble method for the numerical simulation of the Boltzmann equation.

The parton interactions that are included in this work are

$$\begin{aligned} q + q' &\leftrightarrow q + q', & g + g &\leftrightarrow g + g, \\ g + g &\leftrightarrow q + \bar{q}, & g + q &\leftrightarrow q + q. \end{aligned} \quad (4)$$

The cross sections for these processes are leading order (LO) perturbative QCD (LOpQCD) [22] and explicitly

take into account the running coupling constant $\alpha_s(Q^2)$. Since these interaction cross sections diverge, we introduce Debye screening mass $m_D = 0.6$ GeV [16] and quark thermal mass $m_q = 0.2$ GeV in the propagator [30,20]. In principle, those should have the time dependence, we use constant values for simplicity.

The string configuration after parton scattering is determined with a color amplitude similar to the PYTHIA [22]. In Ref. [22], detailed explanations and all possible string configurations are described. Although color connections are screened in a plasma, the string color connections are maintained for the internal consistency of this calculation.

If the energy of the parton-parton scattering is large enough, partons can become off-shell and can radiate. To simulate effectively parton multiplication processes, the time-like branching is included using PYTHIA [23]. This is inspired by the Lund string Monte Carlo to simulate gluon jet productions $e^+e^- \rightarrow q\bar{q}g$. Assuming here that time-like shower approach also works well in the reactions among on-shell partons. The way of the inclusion of the space-time evolution of parton in branching is different from that of the parton cascade model (VNI) by K. Geiger [15]. During the branching, we consider life time of branching partons based on uncertainly principle $t_{form} \sim 1/Q$, where Q is a off-shellness of the partons in the rest frame [35]. Only on-shell partons are propagated in space-time, contrast to the VNI model. In principle, it is important to maintain detailed balance conditions for elementary collisions. We simply neglect the inverse processes like $n \rightarrow 2$, since we are dealing with the expanding system and will not consider the statistical nature of the system.

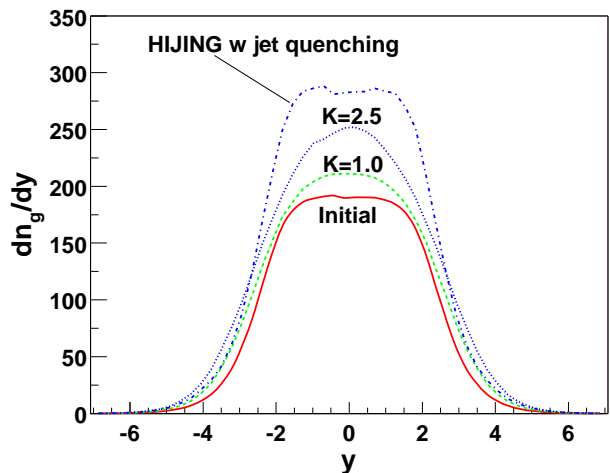


FIG. 1. Rapidity distributions of mini-jet gluons for $Au + Au$ collisions ($b < 4.48$ fm) at $\sqrt{s_{NN}} = 130$ GeV. The solid line denotes the distributions from the initial conditions (HIJING no jet quenching), and the dashed and dotted line represent the distribution after rescattering with K factor of 1.0 and 2.5 respectively. The dotted-dashed line are the result from HIJING default calculation ($dE/dz = 2.0$ GeV/fm).

Taking the momentum space distribution of partons as given by HIJING, the space-time coordinates are calculated using simple uncertainty relations. The formation time for partons are taken to be a Lorentzian distribution with a half width $t = E/m_T^2$, where E and m_T are the parton energy and transverse mass, respectively [21].

In our simulation, the minimum virtuality for the final state radiation is chosen to be 0.5 GeV [35]. The maximum virtuality in parton-parton scattering is assumed to be $Q_{max}^2 = 4p_T^2$, where p_T is transverse momentum transfer of the scattering process. $\alpha_s(Q^2)$ is evaluated at the scale 1 GeV/c, when $p_T < 1$ GeV/c. We use two different parton-parton cross sections using K -factor of 1.0 and 2.5 instead of changing the Debye mass to see the cross section dependence for the parton evolutions. In our case, K -factor of 1.0 yields $\sigma_{gg} \sim 5.3\text{mb}$ for the gluon-gluon cross section, $\sigma_{gq} \sim 2.0\text{mb}$ for the quark-gluon, and $\sigma_{qq} \sim 0.5\text{mb}$ for the quark-quark, respectively. We use $N_{test} = 6$ in the present study. The nuclear shadowing effects in HIJING are included in the all results in this letter.

In Fig. 1, the rapidity distribution of the mini-jet gluons for Au+Au central 10% collision at $\sqrt{s_{NN}} = 130$ GeV are shown. The solid curve represents the initial rapidity distribution of gluons obtained from the HIJING model without jet quenching, where $dN/dy_{g,y=0} = 190$. With this initial gluon number, we obtain the $dN/dy_{g,y=0} = 210$ for K -factor 1.0, and $dN/dy_{g,y=0} = 250$ for K factor 2.5, respectively. On the other hand, HIJING with jet quenching gives us about 280 gluons near mid-rapidity. However, those values are easily changed if different parton-parton cross sections are used.

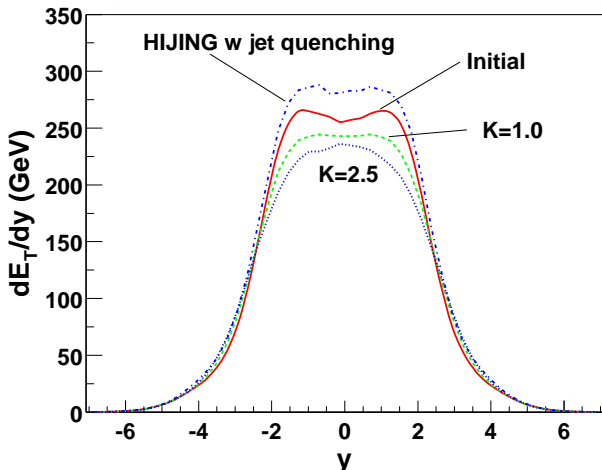


FIG. 2. Transverse energy distributions of partons for Au + Au collisions ($b < 4.48\text{fm}$) at $\sqrt{s_{NN}} = 130$ GeV. The solid line denotes the distributions from the initial conditions and the dashed ($K = 1.0$) and dotted ($K = 2.5$) line represents the distribution after rescattering. HIJING with jet quenching result is shown by the dotted-dashed line.

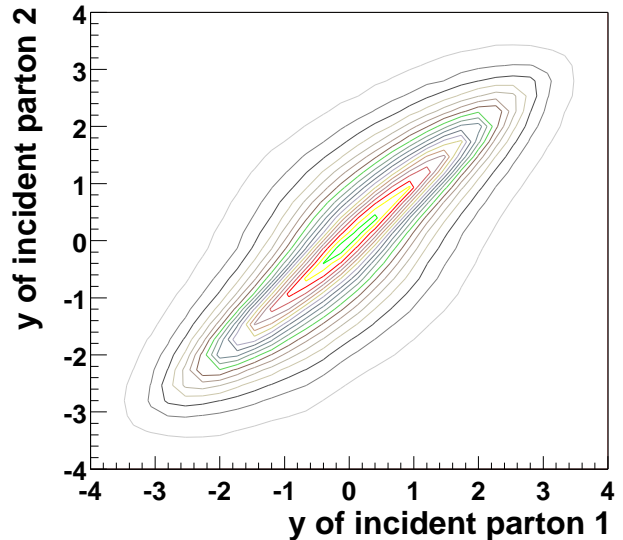


FIG. 3. Rapidity correlation for parton-parton scattering for Au+Au collisions ($b < 4.48\text{fm}$) at $\sqrt{s_{NN}} = 130\text{GeV}$. $K = 2.5$ is used.

In Fig. 2, we show the rapidity distribution of transverse energy dE_T/dy in Au+Au central 10% collisions at $\sqrt{s_{NN}} = 130$ GeV. During the evolutions of partons, transverse energy is reduced about 13GeV ($K = 1.0$), and 27 GeV ($K = 2.5$). while dE_T/dy increases in the HIJING jet quenching scheme. This difference shows clearly that space time evolution of the system is different from that of the assumption of HIJING jet quenching scheme. To see this in more detail, we plot in Fig 3, the rapidity correlation for the parton-parton collisions in the case of $K = 2.5$. The partons with similar rapidities collide each other, partly because the assumption for the initial space-time position for partons yields the Bjorken like correlation. The degree of the correlation depends on the parton-parton cross sections. The correlation is stronger in smaller cross sections. This correlation is absent in HIJING assumption for the jet quenching where the mini-jets above $p_T > 2\text{GeV}/c$ are quenched. Most collisions occur around the p_T of 1.0 GeV/c in our model. When soft collisions of $p_T < 2\text{GeV}/c$ are not included in the simulation, rapidity correlation disappear in our calculations and we have the collision with large rapidity gaps. Therefore, within our model, the collision with high $p_T > 2$ GeV/c is strongly suppressed dynamically.

Fig. 4 shows the gluon transverse momentum distributions from our calculations at the $\sqrt{s_{NN}} = 130$ GeV for central 10% Au+Au collisions together with HIJING calculations. The result of the rescattering including final state radiation (FSR) of the mini-jets is a loss of energy of those at high p_T and a slight increase in the low $p_T < 1$ GeV region. This effects is sensitive to the input parton-parton cross sections.

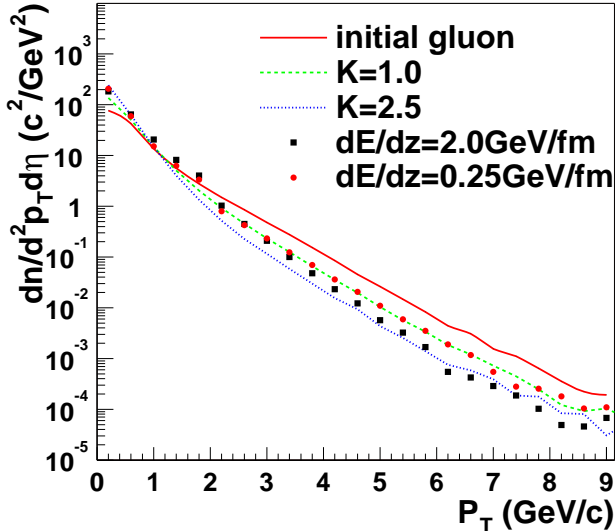


FIG. 4. Transverse momentum distributions of gluons for $Au + Au$ collisions ($b < 4.48\text{fm}$) at $\sqrt{s_{NN}} = 130\text{ GeV}$. The solid line denotes the distributions from the initial conditions and the dashed and dotted lines represent the distribution after rescattering with $K = 1.0$ and $K = 2.5$, respectively. HIJING result are also shown in squares ($dE/dz = 2.0\text{ GeV/fm}$) and circles ($dE/dz = 0.25\text{ GeV/fm}$).

Now we will turn to the comparison of neutral pion spectra which have been measured by PHENIX [1]. Hadrons are obtained from usual Lund string fragmentation scheme [23] keeping in track of the color information during the parton scattering. The color connections are only changed by the parton scattering. Other possible string reconnections are not considered in the present study. As seen in Fig. 5, the result without any final partonic interactions (solid line) overestimates π^0 transverse distribution above $2\text{GeV}/c$, consistent with the pQCD parton model calculations by X.-N. Wang [1,6]. On the other side, any jet quenching effects are not seen in the region of $1 < p_T < 2\text{ GeV}/c$. This is a contrast to the pQCD parton model calculation, which is overestimate in this region without jet quenching. The reason would be that in HIJING, soft interactions are modeled by string formation and it is well tested against the experimental data. However, pQCD parton model is applied down to $p_T \sim 1\text{ GeV}/c$. Above $2\text{GeV}/c$, both HIJING with jet quenching $dE/dz = 0.25 - 2.0\text{ GeV/fm}$ and our simulation reproduce the data well, despite the dynamics of parton system is different from each other. We found that, in order to reproduce the data, $K = 2.5$ is needed. We should mention that the same amount of the quark quenching as the gluon quenching is also necessary to reproduce the PHENIX π^0 data, because at high transverse momentum region $p_T > 4\text{ GeV}/c$ of partons, dominant contributions are quarks and those quarks are converted to the hadrons having the transverse momentum of $p_T \approx 2 - 4$.

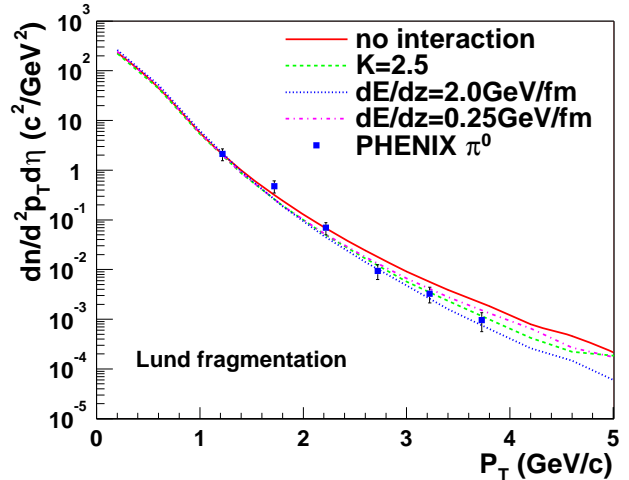


FIG. 5. Comparison of neutral pion transverse momentum distribution for $Au + Au$ collisions ($b < 4.48\text{fm}$) at $\sqrt{s_{NN}} = 130\text{ GeV}$ to the PHENIX data [1]. The solid line denotes the distributions from the initial conditions and the dashed line represents the gluon distribution after rescattering with the K factor 2.5. The HIJING results for $dE/dz = 2.0\text{ GeV/fm}$ (dotted line) and $dE/dz = 0.25\text{ GeV/fm}$ (dotted-dashed line) are also shown.

In the high density partonic system, it would be questionable that the color connections are kept except the two body scattering among mini-jet during the time evolution. We adopt the string picture to model the soft component and neglect their interaction here. In the Lund fragmentation scheme, the strings are fragmented with long-range knowledge of the position of the other jets. In order to see the effects of the long range correlation among strings, we use the independent fragmentation model, in which all partons are fragmented independently. Within this hadronization scheme, π^0 data can be fitted with $K = 1.0$ as shown in Fig. 6. We note that the calculation with $K = 2.5$ cross section underestimates the data. Hadron distributions are more sensitive to the the parton distributions in independent fragmentation model than in the Lund string model. HIJING calculations have the same trend as seen in Fig. [?]. HIJING result with $dE/dz = 2.0\text{ GeV/fm}$ underpredicts the data, while the result with dE/dz is 0.25 GeV/fm fits the data well. This value is the same as that of the pQCD parton model predictions [6].

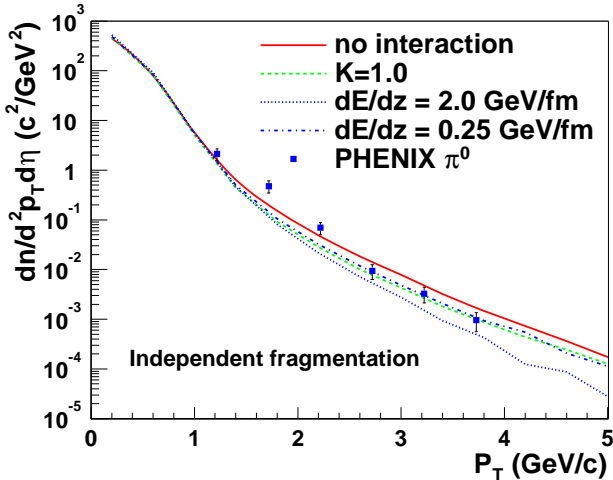


FIG. 6. Comparison of neutral pion transverse momentum distribution for $Au + Au$ collisions ($b < 4.48\text{fm}$) at $\sqrt{s_{NN}} = 130\text{ GeV}$ obtained by the independent fragmentation model to the PHENIX data [1]. The solid line denotes the distributions from the initial conditions and the dashed line represents the distribution after rescattering with the K -factor of 1.0. The HIJING results for $dE/dz = 2.0\text{ GeV/fm}$ (dotted line) and $dE/dz = 0.25\text{ GeV/fm}$ (dotted-dashed line) are also shown. We note that $K = 2.5$ gives us the same amount of underestimation of the data in HIJING result with $dE/dz = 2.0\text{ GeV/fm}$.

Now let us discuss the hadron yield. Recently, PHOBOS reported the incident energy dependence of particle multiplicities [12]. It was shown that HIJING *without* jet quenching is consistent with the energy dependence of charged hadron multiplicity near mid-rapidity. However, π^0 data at $\sqrt{s_{NN}} = 130\text{ GeV}$ can be account for with $dE/dz \approx 0.25 \sim 2.0\text{ GeV/fm}$ in HIJING. One could explain the hadron multiplicity and π^0 data at the same time with different values of dE/dz . The forthcoming data at $\sqrt{s_{NN}} = 200\text{ GeV}$ provides constraints on this effect. Our calculation show that hadron yield near mid-rapidity is smaller (less than 4%) in the case of Lund string fragmentation model and larger (less than 3%) in independent fragmentation model. Our results showed that without increasing the final hadron yield, π^0 above $2\text{ GeV}/c$ spectra can be suppressed. Therefore, our calculations are consistent with the energy dependence of the hadron yield near mid-rapidity.

In this paper we have solved the Boltzmann equation for on-shell partons produced from initial hard scattering given by HIJING initial condition taking relevant LOpQCD processes with final state radiations into account at RHIC energies. We have used two different hadronization model. It is found that π^0 spectra is much more sensitive to the parton distributions in independent fragmentation comparison to the string fragmentation model in which color information among partons are kept and only change when two partons collide. The π^0 data can be reproduced with both models. While the parton-parton interaction increases the parton multiplic-

ity, it modifies the total hadron multiplicity slightly.

We emphasize the importance of the rapidity correlations among interacting partons to suppress the hadron yield. The situation is rather similar with regard to the production mechanism of open charm discussed in Ref. [36]. The space-momentum correlation in secondary parton scattering greatly suppresses the production of charm.

In the present study, soft interactions are modeled by the string formation. We do not consider the final state interactions among those soft color field, because it has been suggested that the high partonic density produced from initial semi-hard scatterings screen the color field. However, string picture itself could be inadequate to describe the high density partonic system at RHIC [32–34,37]. Therefore it is interesting next study to explore the effect of the interactions among soft sector and hard sector replacing the soft sector to incoherent soft partons.

-
- [1] G. David, PHENIX Collaboration, nucl-ex/0105014. talk given at 15th International Conference on Ultrarelativistic Nucleus-Nucleus Collisions (QM2001), Stony Brook, New York, 15-20 Jan 2001.
 - [2] J. P. Blaizot and A. H. Mueller, *Nucl. Phys. B* **289**, 847 (1987). K. Kajantie, P. V. Landshoff, and J. Lindfors, *Phys. Rev. Lett.* **59**, 2527 (1987); K. J. Eskola, K. Kajantie, and J. Lindfors, *Nucl. Phys. B* **323**, 37 (1989).
 - [3] X.-N. Wang and M. Gyulassy, *Phys. Rev. Lett.* **68**, 1480 (1992).
 - [4] M. Gyulassy and X.-N. Wang, *Nucl. Phys. B* **420**, 583 (1994); X.-N. Wang, M. Gyulassy and M. Plumer, *Phys. Rev. D* **51**, 3436 (1995).
 - [5] M. Gyulassy and M. Plumer, *Phys. Lett. B* **243**, 432 (1990).
 - [6] X.-N. Wang, nucl-th/0105053. Talk given at 15th International Conference on Ultrarelativistic Nucleus-Nucleus Collisions (QM2001), Stony Brook, New York, 15-20 Jan 2001.
 - [7] X.-N. Wang and M. Gyulassy, *Phys. Rev. D* **44**, 3501 (1991); X.-N. Wang, *Phys. Rep.* **280**, 287 (1997); X.-N. Wang and M. Gyulassy, *Comp. Phys. Comm.* **83**, 307 (1994).
 - [8] S. E. Vance, M. Gyulassy and X.-N. Wang, *Phys. Lett. B* **443**, 45 (1998); S. E. Vance and M. Gyulassy, *Phys. Rev. Lett.* **83**, 1735 (1999).
 - [9] Z. Lin, S. Pal, C. M. Ko, B. Li and B. Zhang, *Phys. Rev. C* **64**, 011902 (2001).
 - [10] X.-N. Wang and M. Gyulassy, *Phys. Rev. Lett.* **86**, 3496 (2001).
 - [11] B. B. Back, *et al.*, PHOBOS Collaboration, *Phys. Rev. Lett.* **85**, 3100 (2000).
 - [12] B. B. Back, *et al.*, PHOBOS Collaboration, nucl-ex/0108009.

- [13] G. Baym, *Phys. Lett. B* **138**, 18 (1984); K. Kajantie and T. Matsui, *Phys. Lett. B* **164**, 373 (1985); H. Heiselberg and X.-N. Wang, *Phys. Rev. C* **53**, 1892 (1996); G. C. Nayak, A. Dumitru, L. McLerran and W. Greiner, *Nucl. Phys. A* **687** 457 (2001).
- [14] A. H. Mueller, *Phys. Lett. B* **475**, 220 (2000); J. Bjorker, and R. Venugopalan, *Phys. Rev. C* **63** 024609 (2001);
- [15] K. Geiger, *Phys. Rep.* **258**, 238 (1995); *Comp. Phys. Comm.* **104**, 70 (1997).
- [16] B. Zhang, *Comp. Phys. Comm.* **109**, 70 (1997); <http://nt1.phys.columbia.edu/people/bzhang/ZPC/zpc.html>; B. Zhang and Y. Pang, *Phys. Rev. C* **56**, 2185 (1997); B. Zhang, M. Gyulassy and Y. Pang, *Phys. Rev. C* **58**, 1175 (1998).
- [17] D. Molnar and M. Gyulassy, *Phys. Rev. C* **62**, 054907 (2000); nucl-th/0104073.
- [18] S. Cheng *et al.*, nucl-th/0107001.
- [19] E. Shuryak and L. Xiong, *Phys. Rev. C* **49**, 2241 (1994); T. S. Biro, E. van Doorn, B. Müller, M. H. Thoma and X.-N. Wang, *Phys. Rev. C* **48**, 1275 (1993); S. M. Wong, *Nucl. Phys. A* **607**, 442 (1996); R. Baier, A. H. Mueller, D. Schiff and D. T. Son, *Phys. Lett. B* **502**, 51 (2001).
- [20] S. M. Wong, *Phys. Rev. C* **54**, 2588 (1996).
- [21] B. Zhang, C. M. Ko, Bao-AN Li, and Z. Lin, *Phys. Rev. C* **61**, 067901 (2000).
- [22] H.-U Bengtsson, *Comp. Phys. Comm.* **31**, 323 (1984).
- [23] T. Sjöstrand, *Comp. Phys. Comm.* **82**, 74 (1994); PYTHIA 5.7 and JETSET 7.4 Physics and Manual. <http://thep.lu.se/tf2/staff/torbjorn/Welcome.html>.
- [24] S. Loh, C. Greiner, U. Mosel, and M. H. Thoma, *Nucl. Phys. A* **619**, 321 (1997); C. T. Traxler, U. Mosel, and T. S. Biró, *Phys. Rev. C* **59**, 1620 (1999); A. Bonasera, *Phys. Rev. C* **60**, 065212 (1999); A. Bonasera, *Phys. Rev. C* **62**, 052202 (2000).
- [25] G. F. Bertsch and S. Das Gupta, *Phys. Rep.* **150**, 189 (1988).
- [26] G. Welke, R. Malfliet, C. Grégoire, M. Prakash, and E. Suraud, *Phys. Rev. C* **40**, 2611 (1989).
- [27] A. Lang, W. Cassing, U. Mosel, and K. Weber, *Nucl. Phys. A* **541**, 507 (1992).
- [28] A. Lang, H. Babovsky, W. Cassing, U. Mosel, H.G. Reusch and K. Weber, *J. Comp. Phys.* **106**, 391 (1993).
- [29] P. Danielewicz and G. F. Bertch, *Nucl. Phys. A* **533**, 712 (1991).
- [30] G. Kortemeyer, W. Bauer, K. Haglin, J. Murray and S. Pratt, *Phys. Rev. C* **52**, 2714 (1995).
- [31] K. J. Eskola, K. Kajantie, P. V. Ruuskanen and K. Tuominen, *Nucl. Phys. B* **570**, 379 (2000); K. J. Eskola, K. Kajantie and K. Tuominen, *Phys. Lett. B* **497**, 39 (2001).
- [32] A. H. Mueller, *Nucl. Phys. B* **558**, 285 (1999); A. H. Mueller, *Nucl. Phys. B* **572**, 227 (2000); D. Kharzeev and M. Nardi, *Phys. Lett. B* **507** (2001), 121; D. Kharzeev and E. Levin, nucl-th/0108006.
- [33] L. McLerran and R. Venugopalan, *Phys. Rev. D* **49** 2233 (1994); **D49** 3352 (1994); **D50** 2225 (1994).
- [34] A. Krasnitz, and R. Venugopalan, *Nucl. Phys. B* **557**, 237 (1999); *Phys. Rev. Lett.* **84** (2000) 4309; *Phys. Rev. Lett.* **86** (2001) 1717; A. Krasnitz, Y. Nara and R. Venugopalan, hep-ph/0108092.
- [35] K. J. Eskola, X.-N. Wang, *Phys. Rev. D* **49**, 1284 (1994).
- [36] Z. Lin and M. Gyulassy, *Phys. Rev. C* **51**, 2177 (1995); P. Lévai, B. Müller and X.-N Wang, X.-N. Wang, *Phys. Rev. C* **51**, 3326 (1995).
- [37] Z. Lin and C. M. Ko, nucl-th/0108039.